Proceedings of CORROSION/2002
Research Topical Symposium

Microbiologically Influenced Corrosion

Chair: Dr. Brenda Little

Sponsored by the NACE International Research Committee:
P. Andresen, Chair
D. Shoesmith, Vice Chair

NACE International
The Corrosion Society

ISBN: 1-57590-130-7

NACE International
The Corrosion Society
1440 South Creek Drive
Houston, TX 77084-4906

Cover Design: Michele Sandusky, NACE Graphics Department

NACE Press
Manager of NACE Press: Neil Vaughan

www.nace.org

Chemical Characterization of Deposits Associated with Microbiologically Influenced Copper Corrosion in Potable Water Systems

G. G. Geesey
Department of Microbiology, P.O. Box 173520,
Montana State University, Bozeman, MT 59717-3520,
and Biotechnology Department, Idaho National Engineering
and Environmental Laboratory,
P.O. Box 1625, Idaho Falls, ID 83415-2203

A. Baty
Department of Microbiology,
P.O. Box 173520, Montana State University,
Bozeman, MT 59717-3520

P. J. Bremer
New Zealand Institute for Crop & Food Research,
Department of Food Science,
University of Otago, P O Box 56,
Dunedin, New Zealand

P. C. Schamberger
Center for Biofilm Engineering,
P.O. Box 173920, Montana State University,
Bozeman, MT 59717-3980

G. S. Henshaw, B. J. Webster, D. B. Wells
Materials Performance Technologies,
P.O. Box 2225,
Auckland, New Zealand

ABSTRACT

The internal surfaces of copper tubes, removed from potable water distribution systems in Australia and New Zealand, which experienced episodes of copper by-product release or 'blue water,' were evaluated by x-ray photoelectron spectroscopy (XPS) and dynamic secondary ion spectrometry (SIMS). Visual and microscopic inspection of the internal tube surface revealed a mosaic of deposits. Three distinct deposits were identified on the surface of tube recovered from a Grahamtown system in the Hunter Valley (HV) of Australia, whereas two distinct deposits were detected on the surface of tube retrieved from the Defense Scientific Establishment (DSE) facility in Auckland, NZ. XPS analysis revealed the presence of organic nitrogen, with a C/N similar to living biomass, concentrated on the yellow-green surface deposit and the deposit-free area of tube from the HV system. In contrast, deposits and deposit-free areas on the tube from the DSE system contained no significant quantities of organic nitrogen. A secondary ion mass spectrometer (SIMS) depth profile of a corrosion deposit on the surface of tube from the HV system revealed a multi-layer structure, consisting of an organic carbon-enriched $Cu(OH)_2$, $Cu(OH)_2 \cdot CuCO_3$ layer on top of an organic carbon-depleted Cu_2O layer. The structure and chemistry of the surface deposits on the HV tube were consistent with a mechanistic model involving growth of a copper oxide film under neutral or alkaline conditions modified by the presence and activities of surface-associated microorganisms. An alternative mechanism may be responsible for the copper by-product release from the tube in the DSE system, since significant quantities of organic nitrogen were not detected in deposits on tubes from this source. Based on the surface chemical data presented here, it is difficult to determine whether similar mechanisms were responsible for the copper by-product release associated with copper tube from these two different distribution systems. The results do suggest that previous models of copper surface film structure may not describe the range of reactions required to adequately explain copper by-product release under certain conditions.

Keywords: blue water, copper by-product release, microbially influenced corrosion, x-ray photoelectron spectroscopy, secondary ion mass spectrometry

INTRODUCTION

Copper by-product release, cuprosolvency, or 'blue water' in potable water systems constructed of copper tube has been reported in many locations worldwide.[1-4] This condition is characterized by the release of copper as fine particles in plumbing systems distributing soft water in the neutral or neutral-alkaline pH range. "First draw" water may contain between 5 to 300 ppm copper (as Cu^{2+}) as finely suspended precipitates. This phenomenon is distinct from copper corrosion in the presence of water at low pH[5,6] in that it does not significantly compromise the integrity of the tube, but rather leads to copper contamination and coloring of the water. This phenomenon has received increased attention since the implementation of the US EPA Lead-Copper Rule in 1991, which limits total copper in potable water to a maximum of 1.3 mg/L.[7] While copper by-product release may not always occur to the degree that results in 'blue water' (generally requiring concentrations above 5 mg/L), it nevertheless may contribute to a large number of medium-size water utilities in the U.S. to exceed the recommended limit.[8]

The general model of copper dissolution and passivation suggests that the metallic copper/electrolyte interface consist of a protective anodic film. Passive films formed on copper in carbonate containing aqueous solutions have shown that the film has either a single or duplex structure, depending on the electrode potential.[9-12] The duplex film generally consists of an inner layer of Cu_2O and a complex outer layer of CuO, $Cu(OH)_2$ and $CuCO_3$.[9] This film structure is expected to develop rapidly upon exposure of copper to naturally-aerated drinking water.[13] The passive oxide film in simulated potable water has been shown to be composed of Cu_2O (86 %) and CuO (11 %) with the remainder being either $Cu(OH)_2$ or $CuCO_3$.[13] Kinetic measurements of electrochemical passivation demonstrate that at positive cell potentials, rapid nucleation and growth of the outer anodic layers occurs over the top of the Cu_2O layer and that this process takes place concurrently with significant Cu^{2+} dissolution.[14,15] After a short exposure period, the oxide film surface coverage is complete with subsequent thickening of the outer anodic layer. Over long exposure times, the anodic corrosion reaction is controlled by ionic diffusion through the oxide, hydroxide or thermodynamically stable precipitate present at the film/solution interface. Metal cations at the film/solution interface are assumed to be in equilibrium with metal cations in solution and copper solubility in potable water is expected to be controlled by the solubility of species such as CuO, $Cu(OH)_2$ or $Cu_2(OH)_2CO_3$.[16] Copper contamination of soft unbuffered drinking waters ("blue water") over periods of greater than one year is at variance with this general model of copper dissolution and passivity.

Despite extensive studies on the nature of copper oxide films during copper corrosion and passivation, the surface composition and structure of oxide films associated with copper tube experiencing copper by-product release remains poorly understood. While the mechanisms responsible for copper by-product release and its more severe manifestation "blue water" have not been elucidated, the two phenomena are likely related. Proposed mechanisms for copper by-product release include 1) the formation of a silica gel layer, which results in occlusion and accelerated dissolution at anodic sites,[17-19] 2) the presence of a bacterial biofilm and associated acidic extracellular polymeric substances (EPS) that bind copper ions at the metal surface and alter the porosity of the oxide film.[20-23] A mechanism(s) that accounts for the "blue water" phenomenon will not only have to explain the capacity of the bulk aqueous phase to accumulate high concentrations of copper species but will also have to account for the processes of dissolution and occlusion that occur at the copper/electrolyte interface. A better understanding of the mechanisms involved in copper by-product release will lead to the development of more cost effective methods for its prevention or mitigation.

In this paper, we describe the chemical composition and structure of the oxide film on copper tube experiencing copper by-product release. We also discuss the preventive and remedial measures that can be implemented to avoid this phenomenon.

EXPERIMENTAL

Copper Tube Sampling

Sections of copper tube used for distribution of potable cold water were removed from two sites, each of which had experienced episodes of copper by-product release. One section of 22 mm O.D. tubing was recovered from a Grahamtown water system in the Hunter Valley of Australia (HV) that had been in service between 3 and 5 years. Another section of tubing was recovered from a water system in the Defence Scientific Establishment (DSE) in Auckland, New Zealand that had been in service for approximately 24 months. Tube from the Defence Scientific Establishment conformed to NZS 3501:1076, which requires the removal of deleterious carbonaceous surface films. Sections were cut in both cross-section and longitudinally to expose the inner tube surface and associated corrosion deposits for visual and light microscopic, and surface spectroscopic examination. Sections were stored dry until analyzed.

X-ray Photoelectron Spectroscopy

A Physical Electronics Laboratories PHI-5600 X-ray photoelectron spectrometer with a non-monochromatic Al K source operated at 400 watts (15kV, 26.7 mA) was used for the analysis. Samples were analysed at a 45° take-off angle, which equated to a sampling depth of approximately 60 Å. The entrance aperture at the hemispherical energy analyser was set at 4, which equates to an elliptical sampling area with 800 □m as the long axis dimension. Pass energies for the analyser were set at 93.9 eV for wide region survey scans and 58.70 eV for elemental multiplex scans (C1s, O1s, N1s, Cu2p, Zn2p, Si2p, Cl2p, Na1s, In3d). An additional high-resolution scan (5.85 eV) of the Cu2p peak was collected for the copper standards. The peak positions and shakeup bands of different copper compounds were experimentally determined by analysing the following copper standards: Cu_2O, CuO, $Cu(OH)_2$ (Aldrich Chemical Co., Milwaukee, WI) and $CuCO_3 \cdot Cu(OH)_2$ (BDH, Poole, UK) which were pressed into indium foil (Aldrich Chemical Co., Milwaukee, WI) prior to analysis. The operating pressure was typically 5×10^{-8} torr. PHI ACCESS software was employed to collect and display the data, calculate the atomic concentrations from peak areas using a 'Shirley' background. Charge neutralization was accomplished using a beam of 5 eV electrons from an electron gun source. Binding energies were referenced to the adventitious carbon peak at 285.0 eV.

Secondary Ion Mass Spectrometry

Negative ion spectra were acquired at different depths through the HV green corrosion deposit following ion etching using a Cameca 5f secondary ion mass spectrometer with a 10 keV Cs^+ ion beam at a beam current of 110 nA. The 30 μm diameter beam was rastered in a 250 μm x 250 μm pattern. The sample potential was -4.5 keV. The ions were detected with a 60 V offset, except mass 45 (COOH) which had a 0 V offset.

Profilometry

The crater produced through the corrosion deposit by ion etching was profiled using a Rank Taylor Hobson Surtronic 3P profiler with a side skid mounted stylus.

Light Microscopy

Exposed inner tube surfaces were stained with the DNA-binding fluorochrome DAPI, then rinsed with sterile tap water to permit visualization of surface-associated bacteria. The stained tube sections were examined microscopically using an Olympus BMax60 microscope equipped with a 100W mercury lamp and filters optimized for detecting DAPI fluorescence of DAPI-stained bacteria. Unstained surfaces were examined using reflected differential interference contrast (DIC) optics on the same microscope.

RESULTS

Water Chemistry

Table 1 presents the water chemistry determined by each utility responsible for maintaining the quality of the water distributed to each of the potable water systems that experienced copper by-product release. The water in both the HV and DSE systems possessed similar low alkalinity with low buffering capacity. The water in the DSE system in Auckland contained lower total solids, conductivity, hardness, lower chloride, sulfate and sodium concentrations, and higher silica concentrations than water in the HV system of Grahamtown, Australia. The HV system displayed a lower range of pH values than the DSE system.

Copper Tube Surface Features

Microscopic examination of the inner surface of the copper tube recovered from the Grahamtown HV and Auckland DSE systems revealed a heterogeneous mosaic of distinct corrosion deposits. The inner surface of the HV tube contained a yellow-green corrosion product covering approximately 60% of the surface (Figure 1; top, left), under which resided black (Figure 1; top, right) and blue deposits (Figure 1; top, right and bottom, left). The remainder (approximately 30%) of the HV tube surface was brown in color and relatively free of corrosion product (Figure 1; bottom, right). Two deposits were clearly distinguished on the inner surface of the DSE tube: three slightly different shades of a green deposit (blue-green covering 10%, Figure 2; top, left: lavender covering 10%, Figure 2; middle, left: light green covering 20%, middle, right), which together covered approximately 40% of the tubes surface, and a black deposit covering approximately 50% of the surface (Figure 2; top, right). The remainder of the surface (10%) was reddish brown in appearance containing patches of black corrosion deposits (Figure 2, bottom, left). Microscopic examination of the exposed inner tube sections stained with the DNA-binding fluorochrome DAPI revealed bacterial cells non-randomly distributed within the corrosion deposits (data not shown). The bacteria were rod-shaped with dimensions of approximately 5 μm in length and 0.5 μm in width.

X-ray Photoelectron Spectroscopy

The elemental abundance based on XPS survey scans varied among the different corrosion deposits described above (Table 2). Even deposits of similar appearance, but obtained from the different systems, exhibited different elemental abundance. The exceptions were the similar oxygen abundance among the yellow-green, light green, lavender, and blue-green deposits and the similar oxygen abundance among the black deposits from the two different systems (Table 2).

Variations in the $Cu2p_{3/2}$ binding energies suggested that the oxidation state of the copper also varied among the different surface deposits (Table 3). The reddish brown, predominantly deposit-free areas of the Grahamtown HV tube and Auckland DSE tube surfaces displayed $Cu2p_{3/2}$ binding energies of 932.5 eV, indicating the presence of a Cu_2O layer (Table 3). The reddish brown area of the HV tube contained a weak shake-up peak at 944.0 eV, suggesting the presence of CuO, as well (Table 3). The reddish brown area of the DSE tube displayed a stronger shake-up band at 944.0 eV than the corresponding area of the HV tube, suggesting a greater abundance of CuO, possibly corresponding to the black deposits in the bottom, left image of Figure 2. The reddish brown, deposit-free areas of tube recovered from both systems contained a greater abundance of surface carbon and a lower abundance of surface oxygen relative to that detected in any of the accompanying surface deposits. This can be attributed to adventitious carbon adsorbed to the Cu_2O surface in the case of the DSE tube. The significant quantities of nitrogen with N 1s binding energy positioned at 399.7 0.3 eV detected on the reddish brown, deposit-free area on the HV tube, suggests that the carbon, in this case, was organic in nature (Table 2 & 3). The C/N ratio of 8.9 of the reddish brown deposit-free acre on the HV tube is similar to the 7.6 ratio of living biomass in a balanced state of growth.[24]

The yellow-green deposits on the HV tube and the green deposits on the DSE tube consisted of a friable material up to 1 mm thick in some places. The yellow-green deposit was the dominant corrosion product associated with the HV tube. The $Cu2p_{3/2}$ binding energy of Cu associated with the light green deposit on the DSE tube and the blue-green deposit on the HV tube was 932.0/934.8 eV and 934.5 eV, respectively (Table 3). Based on a comparison with binding energies obtained from copper standards, these deposits most closely matched those of $Cu(OH)_2$ and $CuCO_3 \cdot Cu(OH)_2$. The C1s region of these deposits exhibited a peak at 289 eV contributed by the C-O bond arising from the OH groups in a stoichiometry consistent with a carbonate mineral composition (data not shown). This peak was not detected in deposits exhibiting only $Cu(OH)_2$ character.

The blue-green and lavender deposits on the tube recovered from the DSE yielded a $Cu2p_{3/2}$ binding energy of 933.0 eV, which does not coincide with any of the standards evaluated (Table 3). The shake-up peak of these deposits suggest the presence of $Cu(OH)_2$. Addition of Cu_2O to the $Cu(OH)_2$ spectrum could produce a $Cu2p_{3/2}$ peak position similar to that of these deposits, although this was not evaluated experimentally. The C1s band position produced by the lavender deposit, like that produced by the light green deposit on the DSE tube and the yellow-green deposit on the HV tube suggests the presence of carbonate, possibly in the form of $Cu(OH)_2 \cdot CuCO_3$. The crystals associated with the yellow-

green deposits on the HV tube (Figure 1; top, left image), and lavender (Figure 2; middle, left image), and light green (Figure 2; middle, right image) deposits on the DSE tube resemble malachite [$Cu(OH)_2 \cdot CuCO_3$]. The C1s band position produced by the blue-green deposit on the DSE tube suggests little carbonate is present. Likewise, the $Cu2p_{3/2}$ shake-up features of the blue-green deposit do not support the presence of a $Cu(OH)_2 \cdot CuCO_3$ phase (Table 3). The greater abundance of the yellow-green deposit on the HV tube surface compared to that of the deposits over varying shades of green on the DSE tube likely reflects the greater hardness ($CaCO_3$) of the water in the former system (Table 1). Like the reddish brown, deposit-free area, the yellow-green deposit on the HV tube produced a nitrogen signal suggesting the presence of organic nitrogen and a C/N ratio of (7.5) that is also consistent with a living biomass source (Table 2 and 3).[24]

The black on the HV tube occurred as exposed surface deposits and as layers under the green deposit (Figure 1; top, right and bottom, left images). Based on the $Cu2p_{3/2}$ binding energy of 933.8 eV, the black deposit on the HV tube most closely matches CuO (tenorite). The $Cu2p_{3/2}$ binding energy peak for the black deposit on the DSE tube occurred at 932.5 eV, which is indicative of Cu_2O (Table 3). However a shake-up peak was also detected at 943.0 eV in this deposit, which suggests that Cu^{2+} species are present. It is possible that the black deposit on the DSE tube is composed of either a thin (1-2 nm) layer of CuO on top of a Cu_2O film, or islands of CuO on top of Cu_2O.

The blue crystals associated with the blue (Figure 1; bottom, left image) and black deposits (Figure 1; top, right image) on the HV tube, like the black deposits on HV tube, occurred as exposed surface deposits and as layers under the green deposit. The blue crystals are characteristic of $Cu(OH)_2$, but may also be azurite [$2CuCO_3 \cdot Cu(OH)_2$]. Alternatively, the blue deposits may be chloride salts of copper [$Cu_2(OH)_2Cl$ or $CuCl_2 \cdot 3Cu(OH)_2$] since chlorine was also detected at trace levels (Table 2). Authentic standards of these copper salts need to be analyzed and their $Cu2p_{3/2}$ binding energies compared with those obtained from the tube deposits before these assignments are made, however.

The blue deposit was enriched in Si relative to the other deposits (Table 2). The Si2p peak obtained from the blue deposit associated with the HV tube was deconvolved into two components with binding energies centered at 102.5 eV and 103.5 eV, and assigned to silicate and silica, respectively. Although silicate was associated with all the deposits sampled from tube obtained from both systems, only the blue deposit associated with the HV tube displayed a silica band. The carbon associated with the black and blue deposits on the HV tube does not appear to be associated with living biomass since no significant nitrogen signal was recovered from these deposits.

An area of HV tube containing a sharp transition between the reddish brown, deposit-free surface and the yellow-green corrosion deposit was imaged and mapped by XPS to check the chemical assignments made above. XPS survey scans indicate that Zn was uniformly distributed at low abundance across both yellow-green deposit and reddish brown, deposit-free area (Table 4). The results of XPS survey scans, presented in Table 4, also corroborate the elemental abundance presented in Table 2. Similarly, results of the multiplex scans presented in Table 4 support the data presented in Table 3; that CuO and $Cu(OH)_2$ are

enriched in the yellow-green deposit while Cu_2O is only detected in the reddish brown, predominantly, deposit-free areas. Again the C1s and N1s peak positions and relative abundance on both yellow-green deposit and reddish brown, deposit-free area indicated the presence organic carbon with characteristics of living biomass.

Secondary Ion Mass Spectrometry

An ion beam was used to sequentially remove the surface layer of corrosion deposits to expose underlying layers for secondary ion mass spectroscopic (SIMS) analysis. Although the heterogeneous and insulating properties of the deposits introduced surface charging and non-linear etch rates, compromising data quality, negative ion SIMS depth profiles for a number of elements were obtained through the yellow-green corrosion deposit on the HV tube surface. Based on profilometric measurements, the elemental profile extended 30±2 μm through the yellow-green corrosion product into the underlying black and blue corrosion products. Since the Cu abundance at the deepest sample depth was the same as that at much shallower sampling depths, it is unlikely that the profile extended to the base metal.

The parallel changes in abundance with depth of fragments m/e$^-$ 26 and 45, corresponding to CN^- and $COOH^-$, suggests they are derived from a similar source of organic carbon (Figure 3). Furthermore, the profiles identify an organic carbon-rich surface region (region 1), under which resides a region (region 2) that contained an organic carbon content that was 10-20% of that in the region 1 (Figure 3). At greater deposit depths, corresponding to region 3, organic carbon content increased slightly before decreasing to a minimum.

The change in elemental ratios of Cu, O, and Cl with sputter depth also identifies 3 chemically distinct regions (Figure 3). The approximately 5-fold increase in these elements at the boundary of region 1 and 2 corresponded to the depth at which organic carbon decreased an order of magnitude. Over the depth range that Cu abundance remained relatively constant, a 2-fold decrease in Cl abundance in region 2 was followed by a 10-fold decrease in O abundance corresponding to region 3 (Figure 3). Based on the previously described visual inspection results it is likely that regions 1 and 2 contained the yellow-green deposit, while region 3 contained the underlying blue and black deposits. From a cursory understanding of the nature of the different corrosion product layers, the sputter rate through the yellow-green layer is expected to be greater than that through the underlying blue and black layers. Thus, regions 1 and 2 may be 2-3 times thicker than region 3. Since region 2 had lower Cu/Cl and Cu/O ratios than region 3, the former likely contains CuO, $Cu(OH)_2$, and $CuCO_3 \cdot Cu(OH)_2$, while the latter likely contains Cu_2O, supporting assignment of $Cu(OH)_2$, and $CuCO_3 \cdot Cu(OH)_2$ to the yellow-green corrosion deposit, and Cu_2O to the underlying black corrosion deposits, respectively, on the HV tube surface.

DISCUSSION

Calculations of inorganic copper release based on prolonged existence of the thermodynamically metastable $Cu(OH)_2$ phase in combination with copper carbonate phases accurately predict the levels of copper release by a most U.S. water utilities.[25] However, models based solely on inorganic water chemical parameters failed to predict anomalous

cases of copper by-product release in water distribution systems in New Zealand, Australia, U.S.A., Japan and Europe that displayed low alkalinity and buffering capacity, and a pH range of 7.8-9.5.[1,5,8,26-29] In these instances concentrations of total copper in first-draw water from the tap ranged from 2-80 mg/L, which is well above the U.S. EPA maximum contaminant level of 1.3 mg/L.[7]

Systems in the U.S.A., New Zealand and Australia have experienced excess copper by-product release at the extremities of the distribution system where low chlorine residual was common.[3,6,30] Numerous cases of excess copper by-product release in Auckland, New Zealand have been reported in new copper installations, often in dead-legs or in institutional building cold water lines that experienced extended periods of stagnation.[17,29,31] Extended periods of stagnation can occur between the time the system is filled with water and pressure tested and when the building becomes occupied and the water system put into use.

The surface spectroscopic results obtained from the present studies are generally consistent with previously published results in which a CuO-, $Cu(OH)_2$-, and $CuCO_3$-containing surface layer and an underlying Cu_2O-rich layer constitute the "passive film" on copper tube surfaces under neutral to mildly alkaline pH conditions.[32-35] However, visual inspection and XPS of different areas of the surface of copper tube experiencing excess copper by-product release revealed a mosaic of multi-colored, chemically heterogeneous, surface deposits interspersed with corrosion deposit-free areas consisting of Cu_2O that is not commonly associated with stable passive films. Thus, the surface chemistry of tube experiencing copper by-product release appears to be more complex than that of copper tube in systems not experiencing this phenomenon.

The enrichment of N-containing carbon with living microbial biomass character at the surface of the yellow-green deposit and the brown, deposit-free area of the HV tube is different from the graphitic carbon film described by Campbell.[36] The presence of this bacterial biomass may alter the integrity of the yellow-green deposit, contributing to its release into the bulk aqueous phase upon exposure to hydrodynamic shear as proposed by Webster et al.[37] These authors have demonstrated under laboratory conditions that the incorporation of significant microbial biomass into the copper oxide film increases film porosity. Incorporation of microbial biomass also alters the film properties in such a way that it behaves as if it where under more acidic conditions than predicted by the actual pH of the bulk aqueous phase. However, the presence of microbial biomass on the tube surface, by itself, does necessarily cause copper by-product release, since the reddish brown, predominantly, deposit-free areas of the HV tube surface displayed C/N ratios and C 1s and N 1s peak positions similar to those associated with the yellow-green deposits. Thus, some copper films may be more stable in the presence of an attached bacterial population than others. Whether the nature of the copper film determines the composition of the microbial biomass and it properties remains to be determined.

The lack of a significant nitrogen peak in the green surface deposits on the DSE tube suggests that the carbon associated with this deposit was different from that detected on the yellow-green deposit and reddish brown area on the HV tube. The high C/N ratio associated with DSE tube deposits may reflect a source other than microbial biomass carbon, although

some EPS produced by surface-associated microbial populations exhibit low C/N ratios. A high C/N ratio does not exclude the presence of microbial biomass since most surfaces usually contain a thin layer of hydrocarbons adsorbed from the atmosphere during sample preparation. Based on the chemical data presented here, it is difficult to determine whether similar mechanisms were responsible for the copper by-product release associated with copper tube from these two different distribution systems.

Preventive and Remedial Measures for Copper By-Product Release

A variety of factors have been linked to copper by-product release. For example, the problem appears to be more severe in small diameter than large diameter tube, presumably due to the higher surface area to volume ratio.[38] It also occurs more frequently in distribution systems that remain stagnant for extended periods of time between flushing events. Water that is soft, weakly buffered, with neutral to mildly alkaline pH, and low in chlorine residual also can predispose a system to copper by-product release.[25,39] Distribution systems which contain water with elevated levels of dissolved or particulate organic carbon in a state that can be assimilated by microorganisms has also been suggested to predispose a system to undesirable microbial activities such as oxygen removal and biofilm formation.[40] Systems experiencing "blue water" may contain > 100 colony forming units per mL of water due to displacement of biofilm-derived bacteria into the first draw water from the tap during copper by-product release.[41] Oxide film impurities such as foreign particulate material transported to the tube surface by the water and adherent bacterial biofilms that develop in the oxide layer in response elevated levels of organic nutrients in the water alter the structure and increase the porosity of the protective oxide film. The more porous the oxide structure, the higher the corrosion rate.[13,37] Thus, prevention of copper by-product release hinges on the maintenance of a stable, uniform, copper oxide film across the tube surface.

Once a water distribution system experiences copper by-product release, there are a variety of remedial treatments that can be applied to bring the system under control. The first step involves inactivation of the microbial biofilms that have accumulated in the corrosion deposits on the tube surface. This can be accomplished by heat treatment. Webster et al[37] determined that heating a suspension of bacteria, known to cause copper by-product release, to 65 °C killed 90% of the population in 2.4 sec. No bacteria could be cultured after heating for 5 sec at this temperature. Heating the copper surface for periods as long as 10 min had only a minimal effect on the rate of copper corrosion. Consequently, these authors have recommended that in the field, pipes should be exposed to 75 °C water for at least 10 min. Heat treatment seems to be an effective method of killing biofilm bacteria and permitting subsequent removal of the biofilm from the tube surface.

Superchlorination has also been used effectively to kill microbial biofilms responsible for copper by-product release.[37] A 30 ppm shock dose for 4 hrs made the biofilm more susceptible to removal by mechanical means (shear).[41] However, this treatment also increased the corrosion rate by more than an order of magnitude during the superchlorination period and after the dose period allowed a return to corrosion rates similar to those observed prior to treatment. Thus superchlorination alone is not sufficient to remediate the system.

The chemistry of the water introduced into the system following heat treatment or superchlorination also needs to be adjusted so that the pH is slightly above neutral and the buffering capacity sufficient to resist pH excursions at the tube surface.[42,43] Webster et al[41] determined that a tube surface conditioned with water at pH 8 for 81 days, resisted corrosion conditions (pH 5.0), imposed to simulate the presence of a biofilm on the tube surface, better than a tube surface conditioned with water at pH 6.5. Lime is the most common additive to potable water systems for pH adjustment, although caustic soda (NaOH) has also been used due to its ease of handling and storage.[43] A third alternative for elevating the pH of domestic water supplies involves the addition of soda ash (Na_2CO_3), where pH adjustment is desired without the addition of hardness and where insufficient alkalinity is present for stability.[43]

In summary, copper by-product release, cuprosolvency or 'blue water' is a condition that exists in some potable water distribution systems constructed of copper tube where the water displays low buffering capacity and is often depleted of residual chlorine due to prolonged storage in the water lines. Inspection of the inner tube surface revealed a mosaic of corrosion products, some of which were loosely bound to the tube surface and enriched in living biomass. The chemistry of the deposits associated with the HV tube is consistent with a microbial mechanism proposed by Webster et al[37] in which the porosity and corrosion resistance of the film is compromised by an adherent microbial biomass. The absence of significant quantities of organic nitrogen in deposits associated with the DSE tube suggests that mechanisms other than the one proposed by Webster et al[37] may be responsible for copper by-product release in this system. Preventive and remedial measures have been identified that can be applied to control this phenomenon.

ACKNOWLEDGEMENTS

Work reported in this paper was supported by the New Zealand Foundation for Research, Science and Technology under Contract No: CO8516, and by the International Copper Association under Project No. 484. We would like to thank Kathryn Prince, ANSTO, Lucas Heights, Australia for the SIMS analysis.

REFERENCES

1. G.G. Page, MP 11 (1972): p. 53.
2. D.B. Wells, B.J. Webster, P.T. Wilson, P.J. Bremer, "Blue Water Corrosion in Potable Water,"Australasian Corrosion Assoc. Inc. Conference, Corrosion and Prevention, held Nov. 27-30, (Adelaide, Australia: Australasian Corrosion Assoc. Inc., 1994).
3. National Conference on Integrating Corrosion Control and Other Water Quality Goals, held May 19-21, (Cambridge, MA: New England Water Works Association, 1996).
4. Japan Copper Development Association Final Report, TPT-0478, 1994.
5 P. Arens, G.J. Tuschewitzki, M. Wollmann, H. Follner, H. Jacobi, Zbl. Hyg. 196 (1995): p. 444.
6. R.J. Taylor, Interim Report TPT 522/523C (New York, NY: International Copper Association, 1997).

7. Federal Register (56FR 26460), Final Lead and Copper Rule, June 7, 1991.
8 Annonymous, Waterweek, Mar. 29 (1993): p. 5.
9. S. Gonzalez, M. Perez, M. Barrera, A.R. Gonzalez Elipe, R.M. Souto, J. Phys. Chem. B. 102 (1998): p. 5483.
10. H.H. Strehblow, B. Titze, Electrochim. Acta 25 (1980): p 839.
11. W. Kautek, J. G. Gordon, J. Electrochem. Soc. 137 (1990): p 2672.
12. J.C. Hamilton, J. C. Farmer, R. J. Anderson, J. Electrochem. Soc. 133 (1986): p 739.
13. Y. Feng, K.-S. Siow, W.-K. Teo, K.-L. Tan, A.-K. Hsieh, Corrosion 53 (1997): p. 389.
14. M. Perez Sanchez, M. Barrera, S. Gonzalez, R. M. Souteo, R.C. Salvarezza, A.J. Arvia, Electrochim. Acta 35 (1990): p. 1337.
15. M.R.G. Chialvo, R.C. Salvaezza, M.D. Vasques, A.J. Avria, Electrochim. Acta 30 (1985): p. 1501.
16. ANSI/NSF 61-1992, Appendix B, Drinking Water System Components and Health Effects, American National Standards/NSF International Standard, (Ann Arbor, MI: National Sanitation Foundation, 1992).
17. P.C.A. Bailey, "Electrochemical Studies of Copper and Thallium," (Ph.D diss., University of Auckland, NZ: 1972).
18. P.C.A. Bailey, G.A. Wright, Reports on Research Contract to DSIR, Parts I, II, III, (1970).
19. G.G. Page, P.C.A. Bailey, G.A. Wright, Australasian Corr. Engineer. 18 (1974): p. 13.
20. D. Davidson, B. Beheshti, M.W. Mittelman, Biofoul. 9 (1996): p. 279.
21. G.G. Geesey, M.W. Mittelman, T. Iwaoka, P.R. Griffiths, Corrosion/85, paper no. 297 (Houston, TX: NACE International, 1985).
22. P.J. Bremer, G.G. Geesey, Appl. Environ. Microbiol. 57 (1991): p. 1956.
23. B.J. Webster, D.B. Wells, P.J. Bremer, Corrosion/96, paper no: 294, (Houston, TX: NACE International, 1996).
24. A.C. Redfield, B.H. Ketchum, F.A. Richards, "The Sea, Ideas and Observations on Progress in the Study of the Seas," ed. M.N. Hill (New York, NY: Interscience Publ., 1963): p 26.
25. M. Edwards, M.R. Schock, T.E. Meyer, J. AWWA 88 (1996): p. 81.
26. Anonymous, Waterweek, June 7 (1993): p. 3.
27. Anonymous, BIA News 17 (1994): p. 8.
28. Anonymous, Final Report TPT-0478, Japan Copper Develop. Assoc. (1994).
29. E.C. Potter, New Zeal. Plumbers J. 22 (1970): p. 25.
30. G.G. Page, New Zeal. J. Sci. 16 (1973): p. 349.
31. G. Moss, E.C. Potter, CSIRO Concluding Report 1534R, (1984): p. 72
32. U. Bertocci, D.R. Turner, Encyclopedia of the Electrochemistry of Elements, Chap. 2, ed. A.J. Bard (New York, NY: Marcel Dekker Inc, 1974) p. 383
33. W. Kautek, J.G. Gordon, J. Electrochem. Soc. 137 (1990): p. 2672.
34. M. Perez Sanchez, M. Barrera, S. Gonzalez, R.M. Souteo, R.C. Salvarezza, A.J. Arvia, Electrochim. Acta 35 (1990): p. 1337.
35. Y. Feng, W.-K. Teo, K.-S Siow, K.-L. Tan, A.-K. Hsieh, Corr. Sci. 38 (1996): p. 369.
36. H.S. Campbell, J. Inst. Metals 77 (1950): p. 345.
37. B.J. Webster, S.E. Werner, D.B. Wells, P.J. Bremer, Corrosion 56 (2000): p. 942.

38. P.J. Bremer, B.J. Webster, D.B. Wells, J. AWWA 93 (2001): p. 82.
39. M. Edwards, J.L. Ferguson, S.H. Reiber, J. AWWA 86 (1994): p. 74.
40. J.P. Rehring, M. Edwards, Corrosion 52 (1996): p. 307.
41. B.J. Webster, S.E. Werner, D.B. Wells, P.J. Bremer, Proc. New Zealand Water Wastewater Assoc. Ann. Conf. (Wellington, NZ: New Zealand Water Wastewater Assoc., 1998), p.158.
42. A. Cohen, MP 32 (1993): p. 56.
43. A. Cohen, J.R. Myers, MP 32 (1993): p. 43.

Table 1. Chemistry of Grahamtown (Hunter Valley) and DSE (Auckland) potable water

Parameter	Unit	Hunter Valley		DSE	
		Minimum	Maximum	Minimum	Maximum
pH		6.6	7.7	7.1	8.6
Conductivity	$\mu S\ cm^{-1}$	252	325	85	120
Alkalinity	$mg\ L^{-1}\ CaCO_3$	17	27	14	35
Total Hardness	$mg\ L^{-1}\ CaCO_3$	49.7	81.3	20	40
Total Solids	$mg\ L^{-1}$	148	229	55	100
Chloride	$mg\ L^{-1}\ Cl^{-1}$	35	47	9	18
Chlorine	$mg\ L^{-1}\ Cl$	0.4	1.8	0	0.3
Sulphate	$mg\ L^{-1}\ SO_4$	38	49	6	15
Fluoride	$mg\ L^{-1}\ F$	0.85	1.09	0.6	1.3
Total Nitrogen	$mg\ L^{-1}\ N$	0.05	0.07	0	0.3
Iron	$mg\ L^{-1}\ Fe$	0.01	0.29	0	0.2
Aluminium	$mg\ L^{-1}\ Al$	0.045	0.249	0	0.2
Zinc	$mg\ L^{-1}\ Zn$	0.003	0.003	0	0.2
Manganese	$mg\ L^{-1}\ Mn$	0.01	0.06	0	0.05
Silica	$mg\ L^{-1}\ SiO_2$	1.2	3.2	9	15
Sodium	$mg\ L^{-1}\ Na$	22.8	23.3	5	10
Potassium	$mg\ L^{-1}\ K$	0.85	1.96	1	5

Table 2. Relative abundance of elements associated with the surface of corrosion deposits on copper tube recovered from different sites experiencing copper by-product release.

Elemental Abundance %										
Site	**Deposit**	**Cu**	**C**	**O**	**N**	**Si**	**Na**	**Cl**	**Zn**	**C/N**
Grahamtown	Brown	7.9± 0.07	55± 0.14	28± 0	6.2±0.35	1.4±0.14	0.25± 0.21	0.1± 0	1.3±0.07	8.9
	Green	7.3± 0.35	39± 0.35	43± 0.21	5.2±0.07	4.3±0.07	0.1± 0.14	0	0.8±0.07	7.5
	Black	24± 0.07	22± 0.64	48± 0.64	0.8±0	6.0±0	0.1± 0.07	0.1± 0.07	0.2±0.07	>20
	Blue	18± 0.57	11± 0.21	57± 0.07	0.9±0.14	12±0.07	0	0.1± 0.07	0.5±0.28	>10
DSE	Green	14	35	43	1.4	6.0	0	0	0.8	>20
	Black	16	29	45	1.0	7.8	0.1	0	1.0	30
	Lavender	26	28	41	0.5	4.3	0	0.1	0.9	>30
	Blue-green	17	36	41	0.8	4.4	0	0	0.3	>30
	Brown	18	43	34	0.8	3.8	0.2	0.3	0.3	>40

n=2 for Grahamtown samples; n=1 for DSE samples

Table 3. Cu $2p_{3/2}$ binding energies of standards and copper species associated with corrosion deposits

Sample	$Cu2p_{3/2}$	shake-up satellite features
Standards		
Cu_2O	932.5	944.0 weak
CuO	933.7	941.4/943.8
$Cu(OH)_2$	934.9	942.8
$CuCO_3 \cdot Cu(OH)_2$	934.8	942.3
Tube areas/deposits		
Grahamtown HV		
Red/Brown	932.5	944.0 weak
Yellow/Green	934.5	943.0
Black	933.8	942.8
Blue	935.0	943.0
Auckland DSE		
Red/Brown	932.5	944.0
Black	932.5	943.0
Lavender	933.0	943.5
Light green	932.0/934.8	943.5
Blue-green	933.0	943.0

Binding energy positions are ± 0.2 eV.
Peak positions were corrected for sample charging by setting the C1s peak to 285.0 eV.

Table 4. Differences in elemental abundance during transition from yellow-green deposit to reddish brown deposit-free area on HV tube surface

	Elemental Abundance (%)	
Element	Yellow-Green Deposit	Red/Brown Area
O 1s	39.47	26.12
N 1s	6.76	8.04
Zn $2p_3$	0.53	0.53
Si 2p	4.05	1.27
C 1s	43.01	60.82
Cu 2p	6.17	3.23

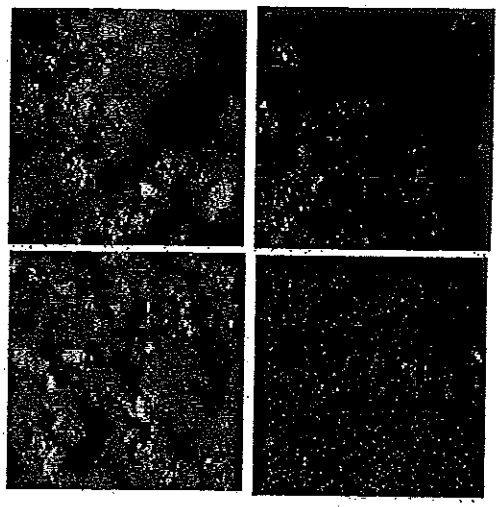

Figure 1. Reflected DIC images of corrosion deposits on inner surface of copper tube recovered from the potable water distribution system in Grahamtown, Hunter Valley, Australia. Yellow-green deposit, top left image; black deposit, top right image; blue deposit, bottom left image, reddish brown area, bottom right image. All images at 100x magnification.

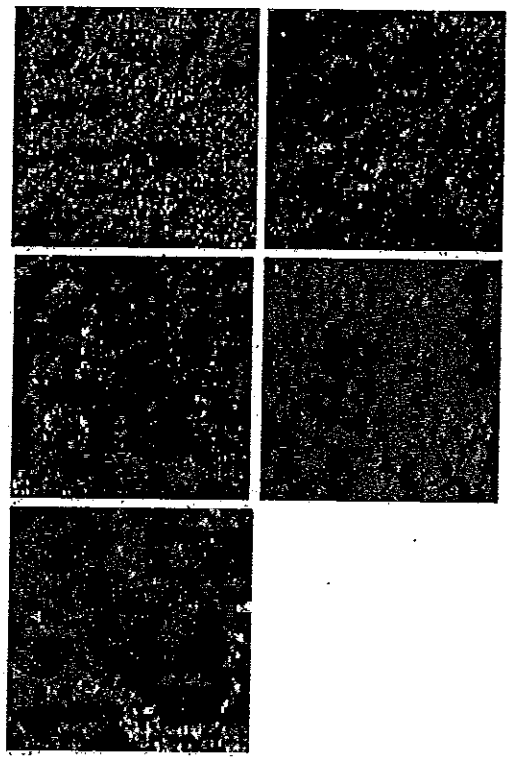

Figure 2. Reflected DIC images of corrosion deposits on inner surface of copper tube recovered from the potable water distribution system in the Defense Scientific Establishment, Auckland. Blue-green deposit, top left image; black deposit, top right image; lavender deposit, middle left image; light green deposit, middle right; reddish brown area, bottom left image. All images at 100x magnification.

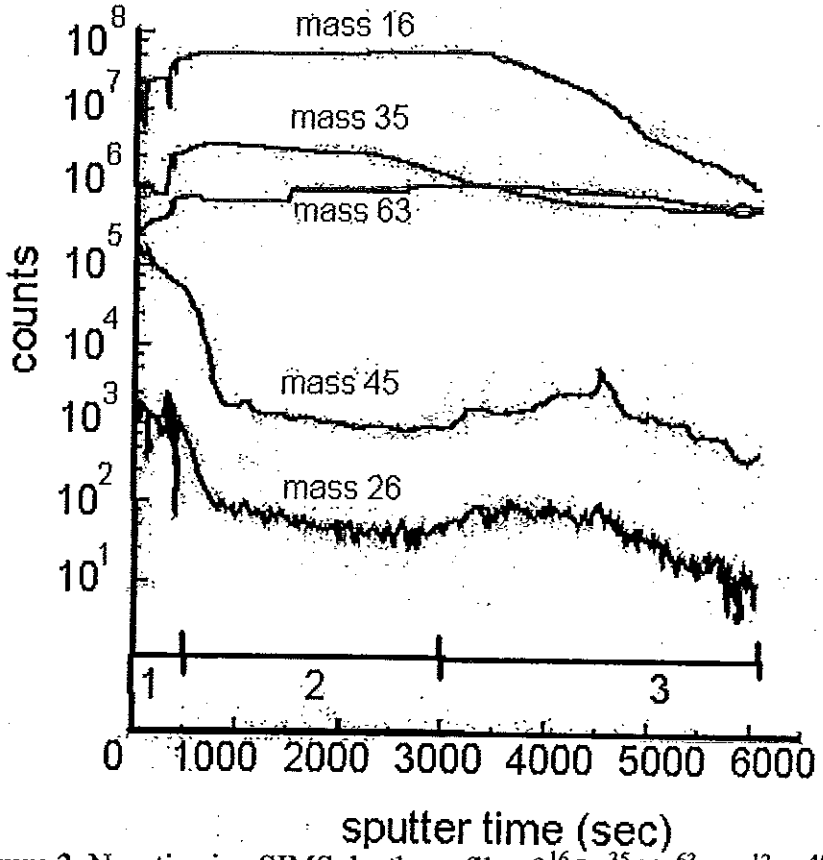

Figure 3. Negative ion SIMS depth profile of ^{16}O, ^{35}Cl, ^{63}Cu, ^{12}C, $^{45}COOH$, and ^{26}CN through the yellow-green deposit on the HV tube surface.